

# Preparation and Crystallization Behavior of Poly(vinylidene fluoride-*ter*-chlorotrifluoroethylene-*ter*-trifluoroethylene)

Hengfeng Li,<sup>1,2</sup> Kaiyuan Tan,<sup>1</sup> Zeming Hao,<sup>1</sup> Guowen He<sup>1</sup>

<sup>1</sup>School of Materials Science and Engineering, Central South University, Changsha 410083, China

<sup>2</sup>State Key Laboratory of Powder Metallurgy, Central South University, Changsha 410083, China

Received 2 March 2010; accepted 30 December 2010

DOI 10.1002/app.34114

Published online 6 July 2011 in Wiley Online Library (wileyonlinelibrary.com).

**ABSTRACT:** Several poly(vinylidene fluoride-*ter*-chlorotrifluoroethylene-*ter*-trifluoroethylene) terpolymers, including 68 mol % vinylidene fluoride, were prepared by the partial reduction of chlorine in poly(vinylidene fluoride-*co*-chlorotrifluoroethylene) copolymers. The terpolymers were then allowed to crystallize under two sets of conditions: (1) crystallized from solution (in *N,N*-dimethylformamide) at 35°C for 108 h and (2) annealed at temperatures 5°C below their respective melting points for 11 h. The effect of the chlorotrifluoroethylene (CTFE) content and crystallization conditions on the crystallization behavior of the terpolymers was investigated by X-ray diffraction, Fourier transform infrared spectroscopy, and differential scanning calorimetry. The results show that with increasing CTFE content, the terpolymers contained less of the  $\beta$  phase (it even disappeared), which had an all-trans chain conformation, and more of the  $\gamma$

phase was found, which became prominent with the trans–trans–trans–gauche conformation. The crystallinity, crystal size, fusion enthalpy, and melting temperatures of the terpolymers decreased with increasing CTFE content. Compared with annealed terpolymers, the terpolymers crystallized from the solution at 35°C included more polar components that contained more trans conformations but had lower crystallinities, melting temperatures, and fusion enthalpies and smaller crystal sizes. These results suggest that crystallization from the solution may be helpful in forming polar crystals, whereas an annealing process at a high temperature is beneficial in perfecting the crystal structure. © 2011 Wiley Periodicals, Inc. *J Appl Polym Sci* 122: 3007–3015, 2011

**Key words:** crystal structures; fluoropolymers; thermal properties; X-ray

## INTRODUCTION

Poly(vinylidene fluoride) (PVDF) and its copolymer with trifluoroethylene (TrFE), poly(vinylidene fluoride-*co*-trifluoroethylene) [P(VDF-*co*-TrFE)], have attracted considerable scientific attention because of their desirable piezoelectric, ferroelectric, and thermoelectric properties and their great potential for advanced applications.<sup>1–9</sup> PVDF and P(VDF-*co*-TrFE) are both semicrystalline polymers. Their polymer chains can be packed into various crystal lattices; this results in different crystalline phases, mainly including the nonpolar  $\alpha$  phase with trans–gauche ( $tg^+tg^-$ ) conformation chains, the polar  $\beta$  phase with all-trans ( $t_{m>4}$ ) conformation chains, and the weakly polar  $\gamma$  phase with trans–trans–trans–gauche ( $ttg^+ttg^-$ ) conformation chains.<sup>1,10</sup> As may be seen in Figure 1, the all-trans conformation chain is a pla-

nar zigzag structure in which the torsional bond arrangement has substituents at approximately 180° to each other, whereas the  $tg^+tg^-$  and  $ttg^+ttg^-$  conformation chains are helical because of the existence of gauche bonds, which have substituents around  $\pm 60^\circ$  to each other. The unit cell of the  $\beta$  phase consists of two  $t_{m>4}$  zigzag chains; its base dimensions are smaller than those of the  $\alpha$  and  $\gamma$  phases, which consist of helical chains.<sup>1,10</sup> Among these crystalline phases, the polar  $\beta$  phase is the most interesting and important because it exhibits a strong ferroelectric behavior. When cooled from the melt, PVDF will crystallize into the  $\alpha$  phase; by mechanical drawing, the  $\alpha$  phase can be converted into the  $\beta$  phase. For the P(VDF-*co*-TrFE) copolymer with vinylidene fluoride (VDF) between 50 and 85 mol %, the  $\beta$  phase can form directly from the melt. One interesting feature of the copolymers in this composition range is the ferroelectric–paraelectric (F–P) transition at a temperature, named the *Curie temperature*, below the melting point of the polymer; this transition is associated with the crystalline form change from the polar  $\beta$  phase to the nonpolar  $\alpha$  phase.<sup>11,12</sup> During the F–P transition, the large chain conformation change between the trans and gauche forms can

Correspondence to: H. Li (lihengfeng@gmail.com).

Contract grant sponsor: National Natural Science Foundation of China; contract grant number: 50703048.

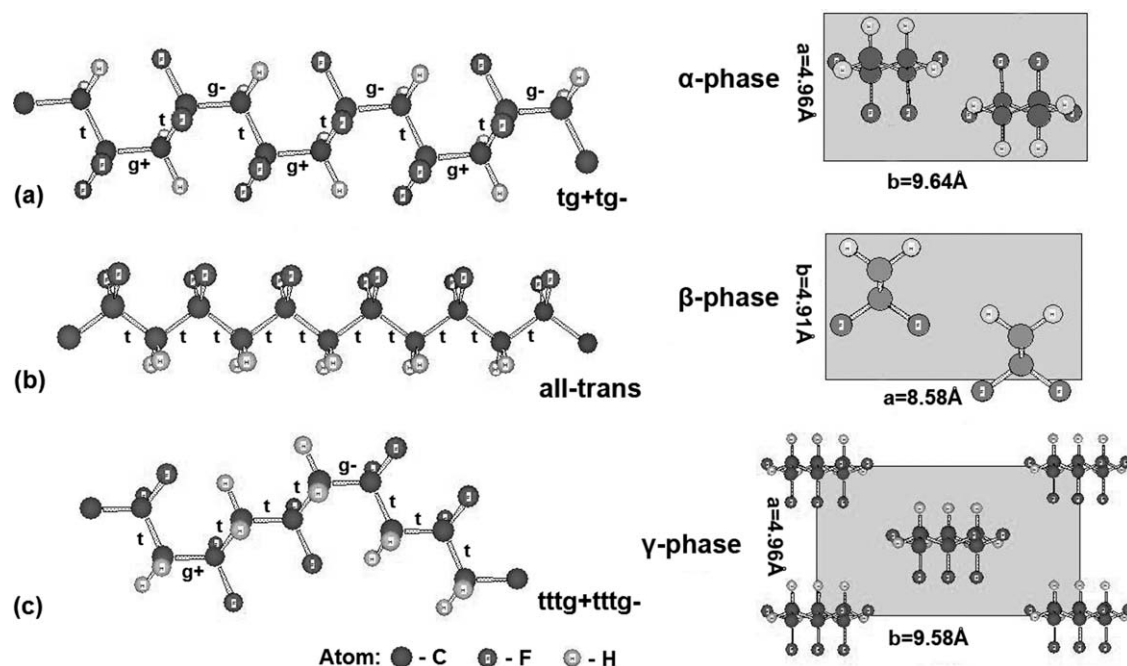


**Figure 1** Schematic depiction of the three most common crystalline chain conformations in PVDF: (a)  $tg^+tg^-$ , (b)  $t_{m>4}$ , and (c)  $ttg^+ttg^-$ . The bonds with substituents at approximately  $180^\circ$ ,  $+60^\circ$ , and  $-60^\circ$  with respect to one another are named t (trans),  $g^+$  (gauche<sup>+</sup>), and  $g^-$  (gauche<sup>-</sup>), respectively. The unit cells of (a) the  $\alpha$  phase, (b) the  $\beta$  phase, and (c) the  $\gamma$  phase of PVDF are shown in a projection parallel to the chain axes.

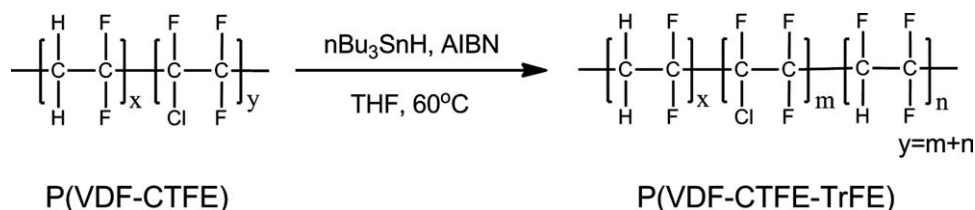
lead to significant changes in the dielectric constant and interesting electromechanical responses. However, the lowest Curie transition temperature for P(VDF-co-TrFE) appears at about  $60^\circ\text{C}$  with 45 mol % TrFE in the copolymer.<sup>12–16</sup> The introduction of a third bulky monomer,<sup>17–21</sup> such as chlorotrifluoroethylene (CTFE), 1,1-chlorofluoroethylene (CFE), or hexafluoropropylene (HFP), as a random defect into P(VDF-co-TrFE) can decrease the energy barrier of the phase transition. The resulting terpolymers exhibit high dielectric constants and large electrostrictive responses at room temperature. Conventionally, the terpolymers are produced by the free-radical polymerization of the three monomers with emulsion, suspension, solution, and bulk methods.<sup>17–21</sup> However, a major concern in these direct processes is the limited supply of the TrFE monomer, which is dangerous in transport and storage and very expensive.<sup>22</sup> Recently, a more convenient chemical route,<sup>23–25</sup> including VDF/CTFE copolymerization and partial reduction of chlorine in poly(vinylidene fluoride-co-chlorotrifluoroethylene) [P(VDF-co-CTFE)], has been reported to synthesize poly(vinylidene fluoride-ter-chlorotrifluoroethylene-ter-trifluoroethylene) [(P(VDF-ter-CTFE-ter-TrFE))] terpolymers, and much work has been focused on their electric storage<sup>26–28</sup> and dielectric properties.<sup>29,30</sup> Despite previous studies on their electric properties, the crystallization behavior of P(VDF-ter-CTFE-ter-TrFE) terpolymers has not been reported in a comprehensive manner.

Although a few studies<sup>25,27,29</sup> have discussed the evolution of the crystalline structures of the terpolymers with their chemical compositions, the influence of the crystallization conditions has been neglected. Moreover, terpolymers with VDF contents below 68 mol % were not included in those studies. In this work, a series of P(VDF-ter-CTFE-ter-TrFE) terpolymers with 68 mol % VDF was prepared via the newly developed approach. The influence of the CTFE content and crystallization conditions on the crystallization behavior of the terpolymers was investigated.

## EXPERIMENTAL

### Materials

Unless otherwise noted, all solvents and reagents were purchased from Nanjing Chemical Reagent Co., Ltd. (Nanjing, China) and were used as received. P(VDF-co-CTFE) was purchased from Chenguang Research Institute of Chemical Engineering (Zigong, China). Gel permeation chromatography measurements in tetrahydrofuran (THF), with polystyrene as a standard, indicated a number-average molecular weight of around  $2 \times 10^5$  g/mol with a polydispersity of about 1.4. Before use, the copolymer was purified by precipitation from the polymer solution in THF with excess methanol. THF was distilled from sodium benzophenone ketyl under nitrogen.



**Scheme 1** Synthetic route for P(VDF-*ter*-CTFE-*ter*-TrFE) terpolymers with various CTFE contents.

### Preparation of the P(VDF-*ter*-CTFE-*ter*-TrFE) terpolymers

As shown in Scheme 1, the P(VDF-*ter*-CTFE-*ter*-TrFE) terpolymers were prepared by the partial reduction of chlorine in P(VDF-*co*-CTFE) copolymers.

P(VDF-*co*-CTFE) copolymer (10.0 g) and 2,2'-azobisisobutyronitrile (AIBN; 1.0 g, 6.0 mmol) were added to a 500-mL, round-bottom flask containing 250 mL of THF. The reaction solution was bubbled with argon for 20 min; this was followed by freeze-pump-thaw cycles and a final argon backfill to provide a positive atmosphere. The mixture was stirred at 60°C for 30 min, and then, Bu<sub>3</sub>SnH (8.0 mL, 28.4 mmol) was added by syringe. The reduction reaction took place at 60°C for 12 h before it was quenched with methanol. After the solvents were evaporated, the resulting precipitate was washed with hexane and dried *in vacuo* to yield 9 g of P(VDF-*ter*-CTFE-*ter*-TrFE) as a white solid. We removed the tin byproducts by dissolving the polymer in a large quantity of THF and then allowing the solution to go through a stationary phase composed of 10% w/w finely ground KF and 90% w/w silica.<sup>31</sup> Finally, the terpolymer was further purified by precipitation in methanol.

According to the procedures mentioned previously, several reactions were carried out. The reaction conditions are listed in Table I.

### Crystallization of the P(VDF-*ter*-CTFE-*ter*-TrFE) films

The predetermined amounts of polymers were fully dissolved in *N,N*-dimethylformamide (DMF) to make some homogeneous solutions with concentrations of 100 mg/mL. The solutions were poured onto clean glass slides and dried *in vacuo* at 35°C for 108 h. Polymer films were obtained.

The polymer films were heated to a temperature sufficient to melt the crystals. They were then allowed to anneal at temperatures about 5°C below their respective melting temperatures, as determined by differential scanning calorimetry (DSC), for 11 h. The polymer films were subsequently cooled in air at a moderate rate.

### Characterization

<sup>1</sup>H-NMR and <sup>19</sup>F-NMR spectra were recorded on a Bruker AM-300 spectrometer instrument (Bruker Corporation, in Karlsruhe, Germany) with acetone-*d*<sub>6</sub> as a solvent. The molecular weights of the polymers were characterized with a Viscotek gel permeation chromatography system (Viscotek Corporation, in Houston, Texas) in a THF mobile phase at a flow rate of 1.0 mL/min; linear polystyrenes were used as calibration standards. A Jena Multi EA 4000 elemental analyzer (Analytic Jena AG, in Jena, Germany) was used to determine the chlorine content of

**TABLE I**  
Reductive Reaction Conditions and Polymer Compositions

Reaction <i>i</i>	Reaction conditions				Polymer <i>j</i>	Chlorine content (wt %) <sup>a</sup>	Polymer composition (mol %) <sup>b</sup>		
	P(VDF- <i>co</i> -CTFE) (10.0 g/123.8 mmol)	Bu <sub>3</sub> SnH (mmol)	AIBN (mmol)	Time (h)			VDF	CTFE	TrFE
					0	14.1	68.0	32.0	0
1	123.8	28.4	6.0	12	1	6.0	68.0	13.6	18.4
2	123.8	42.6	9.0	18	2	3.0	68.0	6.7	25.3
3	123.8	56.8	12.0	24	3	1.9	68.0	4.4	27.6
4	123.8	71.0	15.0	30	4	0.5	68.0	1.1	30.9

The mother P(VDF-*co*-CTFE) copolymer is labeled polymer 0 (*j* = 0); the ultimate product of reaction *i* is labeled polymer *j* (*j* = *i*).

<sup>a</sup> Determined by elemental analysis.

<sup>b</sup> Average of values based on the NMR spectra and the results calculated with the weight percentage of chlorine.

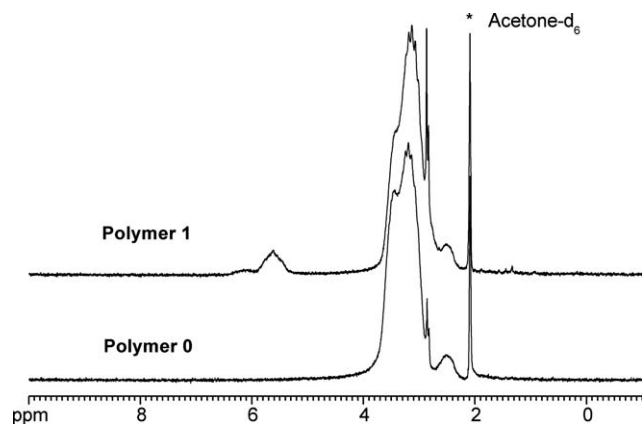


**Figure 2**  $^1\text{H-NMR}$  spectra of the P(VDF-*co*-CTFE) copolymer (polymer 0) and its partial reduction product, the P(VDF-*ter*-CTFE-*ter*-TrFE) terpolymer (polymer 1), in reaction 1 (acetone- $d_6$  was used as a solvent).

the polymers by a microcoulometry method; the analyzer had flame sensor technology and a unique coulometric detection system to ensure highly precise measurement results. X-ray diffraction (XRD) measurements were performed with a Rigaku 2500 D-max diffractometer (Rigaku Corporation, in Tokyo, Japan) with a 1.54-Å wavelength. The (200,110) diffraction peak associated with interchain spacing perpendicular to the polymer chain was determined with a reflection scan. Room-temperature Fourier transform infrared (FTIR) spectra were collected with a Nicolet 6700 spectrometer (ThermoNicolet Corporation, in Madison, Wisconsin) the wave-number range was set from 400 to 1600  $\text{cm}^{-1}$ , with a resolution of 4  $\text{cm}^{-1}$  and an interval of 1  $\text{cm}^{-1}$ . Samples for FTIR analysis were made by the casting of the polymer solution on KBr windows, where they underwent the same conditions as the samples for other characterizations. The DSC study was conducted with a Netzsch DSC 200 F3 thermal analyzer (NETZSCH Group, in Selb, Germany). To compare the influence of different conditions on crystallization behavior of the terpolymer, the first heating ramp was recorded. The temperature of the instrument was calibrated with indium and lead standards. For heat flow calibration, the same indium sample was used. The sample was hermetically sealed in an aluminum pan and heated from 10 to 200°C at a rate of 10°C/min. The typical sample size for DSC was 10 mg.

## RESULTS AND DISCUSSION

### Chemical structures and compositions of the polymers

Figure 2 shows the  $^1\text{H-NMR}$  spectra of the mother P(VDF-*co*-CTFE) copolymer (polymer 0) and its partial reduction product, P(VDF-*ter*-CTFE-*ter*-TrFE) terpolymer (polymer 1), in reaction 1. The structures of polymers 0 and 1 identified by  $^1\text{H-NMR}$  are listed as follows:

(1) polymer 0: 2.7–3.7 (m, 2H,  $-\text{CF}_2\text{CH}_2\text{CF}_2\text{CH}_2-$ , head-to-tail structure of the VDF segment) and 2.2–2.6 (m, 2H,  $-\text{CF}_2\text{CH}_2\text{CH}_2\text{CF}_2-$ , tail-to-tail structure of VDF segment), and (2) polymer 1: 5.3–5.8 (m, 1H,  $-\text{CFHCF}_2-$  of the TrFE segment), 2.7–3.7 (m, 2H,  $-\text{CF}_2\text{CH}_2\text{CF}_2\text{CH}_2-$ , head-to-tail structure of VDF segment), and 2.2–2.6 (m, 2H,  $-\text{CF}_2\text{CH}_2\text{CH}_2\text{CF}_2-$ , tail-to-tail structure of the VDF segment).<sup>7,8,25</sup> The appearance of the signals around 5.6 ppm in the  $^1\text{H-NMR}$  spectrum of polymer 1, which corresponded to the protons from TrFE, confirmed the transformation of the P(VDF-*co*-CTFE) copolymer into the P(VDF-*ter*-CTFE-*ter*-TrFE) terpolymer via the reductive reaction. No residual tin byproducts were found in the purified reductive products.

Figure 3 shows the  $^{19}\text{F-NMR}$  spectra of polymers 0 and 1. The  $^{19}\text{F-NMR}$  spectrum of polymer 0 showed three major chemical shifts at  $-92$  to  $-97$ ,  $-106$  to  $-111$ , and  $-120$  to  $-122$  ppm, which mainly corresponded to three fluorine species:  $-\text{CH}_2\text{CF}_2-$ ,  $-\text{CF}_2\text{CFCl}-$ , and  $-\text{CF}_2\text{CFH}-$  (with bold letters), respectively.<sup>23–25,32</sup> After reduction, the chemical shifts associated with the CTFE units ( $-106$  to  $-111$  and  $-120$  to  $-122$  ppm) become weaker, and a new chemical shift related to TrFE ( $-\text{CF}_2\text{CFH}-$ ) at about  $-200$  ppm emerged. Details of the  $^{19}\text{F-NMR}$  chemical shifts and their corresponding structures are listed in Table II.<sup>23–25,32</sup> The chemical compositions of the polymers could be calculated from the integrals of the characteristic peaks in  $^{19}\text{F-NMR}$  and  $^1\text{H-NMR}$  spectra according to the method described in the literature.<sup>23–25</sup> In this work, we attempted to determine the compositions of the polymers on the basis of their chlorine content (measured by chlorine analysis): polymer 0 only contained VDF and CTFE units, and no chlorine existed in the VDF units. Therefore, its molar composition could be calculated by the following formula:

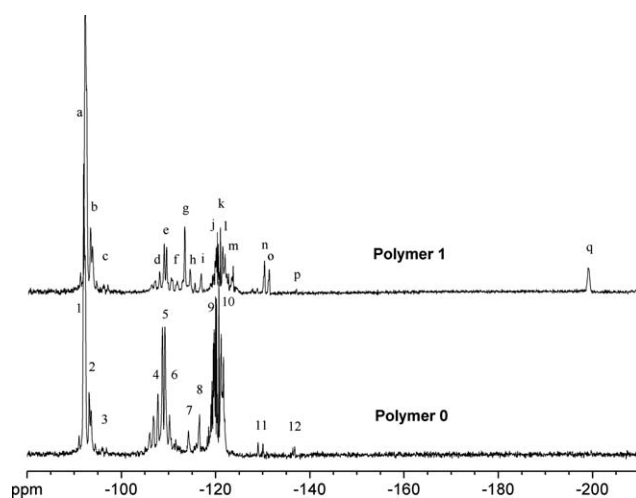


**Figure 3**  $^{19}\text{F-NMR}$  spectra of the P(VDF-*co*-CTFE) copolymer (polymer 0) and its partial reduction product, the P(VDF-*ter*-CTFE-*ter*-TrFE) terpolymer (polymer 1), in reaction 1 (acetone- $d_6$  was used as a solvent).

TABLE II  
Chemical Shifts and Assignments of the <sup>19</sup>F-NMR Peaks for Polymers 0 and 1

Polymer 0			Polymer 1		
Peak	Chemical shift (ppm)	Structure	Peak	Chemical shift (ppm)	Structure
1	-92.0	-CF <sub>2</sub> CH <sub>2</sub> CF <sub>2</sub> CH <sub>2</sub> CF <sub>2</sub> -	a	-92.1	-CF <sub>2</sub> CH <sub>2</sub> CF <sub>2</sub> CH <sub>2</sub> CF <sub>2</sub> -
2	-92.9 to -93.8	-CFCICH <sub>2</sub> CF <sub>2</sub> CH <sub>2</sub> CF <sub>2</sub> -	b	-93.0 to -93.9	-CHFCH <sub>2</sub> CF <sub>2</sub> CH <sub>2</sub> CF <sub>2</sub> -
3	-94.2 to -97.3	-CH <sub>2</sub> CH <sub>2</sub> CF <sub>2</sub> CH <sub>2</sub> CF <sub>2</sub> -	c	-94.2 to -97.3	-CH <sub>2</sub> CH <sub>2</sub> CF <sub>2</sub> CH <sub>2</sub> CF <sub>2</sub> -
4	-105.6 to -107.9	-CF <sub>2</sub> CFCICF <sub>2</sub> CFCICF <sub>2</sub> -	d	-105.4 to -107.9	-CF <sub>2</sub> CFCICF <sub>2</sub> CFCICF <sub>2</sub> -
5	-108.1 to -109.5	-CF <sub>2</sub> CH <sub>2</sub> CF <sub>2</sub> CF <sub>2</sub> CFCI-	e	-108.2 to -109.7	-CF <sub>2</sub> CH <sub>2</sub> CF <sub>2</sub> CF <sub>2</sub> CFCI-
6	-109.5 to -113.0	-CF <sub>2</sub> CFCICF <sub>2</sub> CFCICH <sub>2</sub> -	f	-109.8 to -112.2	-CF <sub>2</sub> CFCICF <sub>2</sub> CFCICH <sub>2</sub> -
7	-114.2	-CF <sub>2</sub> CH <sub>2</sub> CF <sub>2</sub> CF <sub>2</sub> CH <sub>2</sub> -	g	-112.9 to -113.1	-CF <sub>2</sub> CH <sub>2</sub> CF <sub>2</sub> CF <sub>2</sub> CHF-
8	-116.5	-CH <sub>2</sub> CF <sub>2</sub> CF <sub>2</sub> CH <sub>2</sub> CH <sub>2</sub> -	h	-114.3	-CF <sub>2</sub> CH <sub>2</sub> CF <sub>2</sub> CF <sub>2</sub> CH <sub>2</sub> -
9	-118.3 to -120.0	-CH <sub>2</sub> CF <sub>2</sub> CF <sub>2</sub> CFCICH <sub>2</sub> -	i	-116.6	-CH <sub>2</sub> CF <sub>2</sub> CF <sub>2</sub> CF <sub>2</sub> CH <sub>2</sub> -
10	-120.5 to -122.9	-CF <sub>2</sub> CF <sub>2</sub> CFCICH <sub>2</sub> CF <sub>2</sub> -	j	-119.0 to -119.7	-CH <sub>2</sub> CF <sub>2</sub> CF <sub>2</sub> CFCICH <sub>2</sub> -
11	-129.0 to -130.0	-CF <sub>2</sub> CH <sub>2</sub> CFCICF <sub>2</sub> CH <sub>2</sub> -	k	-120.9	-CF <sub>2</sub> CF <sub>2</sub> CFCICH <sub>2</sub> CF <sub>2</sub> -
12	-136.1 to -137.0	-CH <sub>2</sub> CF <sub>2</sub> CFCICF <sub>2</sub> CH <sub>2</sub> -	l	-121.3 to -121.8	-CF <sub>2</sub> CHF <sub>2</sub> CF <sub>2</sub> CHF <sub>2</sub> -
			m	-123.5	-CF <sub>2</sub> CHF <sub>2</sub> CF <sub>2</sub> CHF <sub>2</sub> -
			n	-130.0	-CH <sub>2</sub> CF <sub>2</sub> CF <sub>2</sub> CHF <sub>2</sub> -
			o	-131.1	-CF <sub>2</sub> CFCICF <sub>2</sub> CHF <sub>2</sub> -
			p	-137.0	-CH <sub>2</sub> CF <sub>2</sub> CFCICF <sub>2</sub> CH <sub>2</sub> -
			q	-198.7	-CF <sub>2</sub> CF <sub>2</sub> CF <sub>2</sub> CH <sub>2</sub> CF <sub>2</sub> -

$$\begin{aligned} &(\text{VDF})_0/(\text{CTFE})_0 \\ &= \frac{1 - M_{\text{CTFE}}(W_{\text{Cl}})_0/M_{\text{Cl}}}{M_{\text{VDF}}} \bigg/ \frac{M_{\text{CTFE}}(W_{\text{Cl}})_0/M_{\text{Cl}}}{M_{\text{CTFE}}} \quad (1) \end{aligned}$$

where (VDF)<sub>0</sub> and (CTFE)<sub>0</sub> are the molar percentages of the VDF and CTFE units, respectively, in polymer 0;  $M_{\text{Cl}}$  is the atomic weight of chlorine (35.5);  $M_{\text{VDF}}$  and  $M_{\text{CTFE}}$  are the formula weights of the VDF (64) and CTFE units (116.5), respectively; and  $(W_{\text{Cl}})_0$  is the weight percentage of chlorine in polymer 0. For polymer *j*, the composition could be calculated with the following formulas:

$$(\text{VDF})_j = (\text{VDF})_0 \quad (2)$$

$$(\text{CTFE})_j = (W_{\text{Cl}})_j (\text{CTFE})_0 / (W_{\text{Cl}})_0 \quad (3)$$

$$(\text{TrFE})_j = (\text{CTFE})_0 - (\text{CTFE})_j \quad (4)$$

where (VDF)<sub>*j*</sub>, (CTFE)<sub>*j*</sub>, and (TrFE)<sub>*j*</sub> are the molar percentages of the VDF, CTFE, and TrFE units, respectively, in polymer *j*, and  $(W_{\text{Cl}})_j$  is the weight percentage of chlorine in polymer *j*. Because of the high purity of the polymers, the composition results from this method agreed well with those from the <sup>19</sup>F-NMR and <sup>1</sup>H-NMR spectra. In Table I, the polymer composition, an average of the values based on these two methods, is given.

### XRD analysis

Figure 4 shows the room-temperature (200,110) XRD peaks for the polymers under two crystallization conditions. To make a detailed analysis, each peak

was fitted with a Lorentzian function by Jade 5.0 software (Rigaku Corporation, in Tokyo, Japan). In the fitting process, a linear background was deleted. The fitting results are summarized in Table III.

The room-temperature (200,110) XRD peak from the β phase of the P(VDF-*co*-TrFE) (68/32 mol %) copolymer was reported to be at a 2θ value of 19.80° approximately,<sup>33,34</sup> which corresponded to an inter-chain lattice spacing of 0.448 nm. On the basis of the fitting results in Table III, we found that all of the diffraction peaks of the terpolymers stood at the angles lower than 19.80°. From polymer 4 to polymer 1, the 2θ value progressively became smaller; this indicated a larger interchain spacing and gradual disappearance of the compact structure (polar β phase) with increasing CTFE content of the terpolymer. This was because polymer chains in the crystals of the terpolymers had to adjust their spacing to accommodate the large van der Waals radius of chlorine in the CTFE units. Moreover, the random distribution of chlorine along the chains was favorable to the introduction of kinks (with gauche conformation) into the otherwise planar zigzag *t*<sub>*m*>4</sub> chain conformation.<sup>19</sup> As a result, with the introduction of CTFE units, the closely packed planar zigzag chains with *t*<sub>*m*>4</sub> conformations in the β phase of P(VDF-*co*-TrFE) were converted into more loosely packed helical chains with *t*t<sub>*g*</sub><sup>+</sup>t<sub>*g*</sub><sup>-</sup> and/or *t*<sub>*g*</sub><sup>+</sup>*t*<sub>*g*</sub><sup>-</sup> conformations in the P(VDF-*ter*-CTFE-*ter*-TrFE) terpolymers. This conversion was associated with the crystalline form changing from the polar β phase to the weakly polar γ phase and/or the nonpolar α phase. On the basis of the sum of the areas of crystalline peaks from the fitting data, the degree of crystallinity could be estimated. The crystallinity

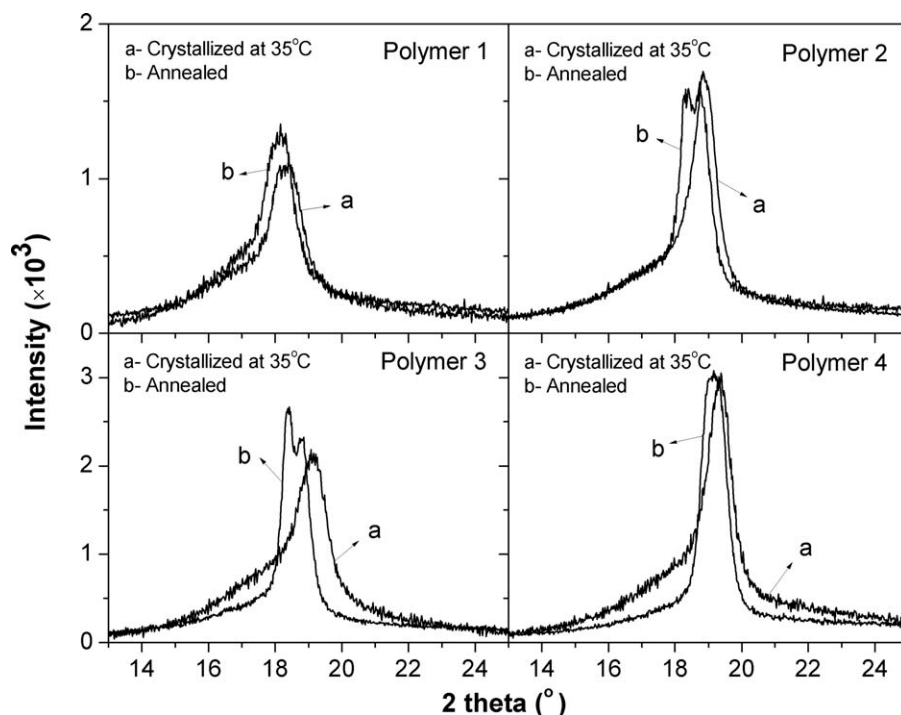


Figure 4 Room-temperature (200,110) XRD peaks of polymers 1–4 crystallized under two sets of conditions.

decreased with an increase in the CTFE concentration of the polymers for both crystallization conditions. This demonstrated that the CTFE unit, as the role of defect, destroyed the crystalline structures of the polymers. All of the results were consistent with the data obtained from other P(VDF-*ter*-CTFE-*ter*-TrFE) terpolymers with VDF contents above 68 mol %.<sup>25,27,29</sup>

The diffraction peaks for annealed polymers 2 and 3 are shown as two resolved peaks. Their fitting data contained two crystalline regions for each peak. Because in the DSC curves of annealed polymers 2

and 3 (given in the DSC analysis), both had two melting peaks, it was reasonable to believe that two types of crystals existed in each of the two polymers. One was formed during the isothermal process, whereas the other was formed during the cooling process. For the annealed polymer 1 and all of the polymers crystallized at 35°C (especially, polymers 3 and 4, crystallized at 35°C), their diffractograms had bulgier shoulders in the left side, which implied that more than one type of crystalline form coexisted in the polymers. So their fitting data had two

TABLE III  
Summary of the Data for the Peak Fitting of the (200,110) X-Ray Reflections of the Polymers

Polymer j	Structural region	Crystallized at 35°C					Annealed				
		2θ (°)	Height	Area (%)	Full width at half-maximum (°)	$L_{200,110}$ (nm)	2θ (°)	Height	Area (%)	Full width at half-maximum (°)	$L_{200,110}$ (nm)
1	Crystalline	17.16	75	1.8	1.53	5.3	16.84	57	1.3	1.45	5.5
		18.33	654	11.4	1.07	7.5	18.17	801	18.4	1.05	7.7
2	Amorphous	16.96	203	86.8	9.73	NA	16.87	220	80.3	8.97	NA
		18.01	73	3.3	1.35	6.0	18.3	1053	18.1	0.48	16.8
3	Crystalline	18.91	1101	28.3	0.79	10.2	18.77	906	13.2	0.54	14.9
		17.22	318	68.4	5.47	NA	17.2	291	68.7	4.79	NA
4	Amorphous	17.81	317	13.1	2.74	2.9	18.35	1964	25.6	0.42	19.2
		19.17	1396	21.3	0.96	8.4	18.82	1462	18.3	0.46	17.6
4	Crystalline	18.49	402	65.6	9.32	NA	17.54	314	56.1	4.01	NA
		18.12	183	5.2	1.55	5.2	19.15	2706	60.4	0.77	10.5
4	Amorphous	19.36	2393	37.1	0.83	9.7	17.95	249	39.6	4.85	NA
		17.89	407	57.7	7.29	NA					

NA, not available.

crystalline peaks for each: one higher angle peak with a larger area and one lower angle peak with a smaller area. On the basis of the results of FTIR analysis (given in the next section), which suggest that the  $\text{tttg}^+\text{tttg}^-$  conformation dominated the polymer chains, it was reasonable to link the higher angle peaks to the crystalline regions dominated by the  $\gamma$  phase and the lower angle peaks to the crystalline regions dominated by the  $\alpha$  phase. In general, the polymers crystallized from the solution at 35°C had higher degrees of diffraction angles but a lower degree of crystallinity compared with the corresponding annealed ones. A reasonable explanation for this may be that in the solution, dipole interactions between the solvent (DMF) could expand the random chain coils to obtain polymer chains, including less helical structures;<sup>35</sup> this led to closer packing of the chains containing more trans conformation in the crystals. Better molecular mobility when it was annealed at a higher temperature made the crystal structure easier to perfect.

The crystallite size or coherence length perpendicular to a particular crystallographic plane ( $L_{hkl}$ ) can be estimated with the Scherrer equation:

$$L_{hkl} = \frac{0.9\lambda}{B \cos \theta} \quad (5)$$

where  $\lambda$  is the X-ray wavelength,  $B$  is the full width at half-maximum of the reflection peak (radians), and  $\theta$  is the diffraction angle. Table III lists the coherence lengths for the (200,110) reflection of the polymers. The polymers crystallized at 35°C had relatively short coherence lengths, which elongated after annealing at a higher temperature. This was probably because the mobility of polymer chains was not high enough to form large crystal structures at low temperature. After annealing, the coherence length substantially grew in polymers 2 and 3. However, only a slight growth was apparent in polymers 1 and 4. This may have been because polymer 1 had too many CTFE units as defects, which were adverse to crystal growth, and polymer 4 contained a relatively higher concentration of polar components. The polarization domain size of polymer 4, which was normally much smaller than the crystallite size, limited the coherent X-ray reflection length.<sup>13</sup>

### FTIR analysis

The FTIR spectra of the polymers at room temperature were obtained to study their chain conformation. As shown in Figure 5, the absorption bands at 1290, 505, and 614  $\text{cm}^{-1}$  arose from the vibration of the  $\text{CF}_2$  group in the  $\text{t}_{m>4}$ ,  $\text{tttg}^+\text{tttg}^-$ , and  $\text{tg}^+\text{tg}^-$  conformation polymer chains, respectively.<sup>36,37</sup> It was clear that the  $\text{tttg}^+\text{tttg}^-$  conformation of the  $\gamma$  phase

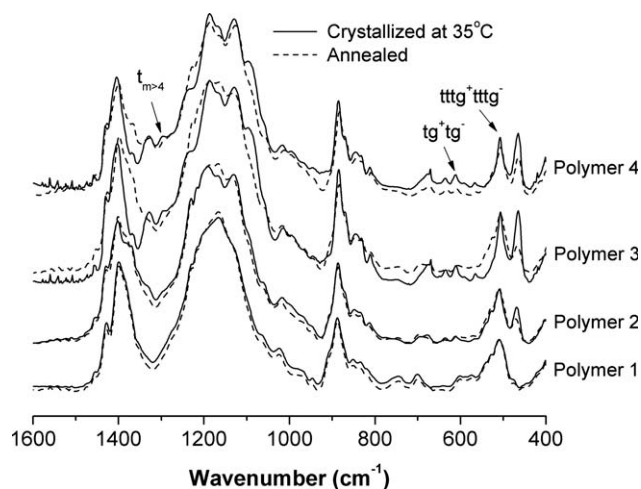


**Figure 5** Room-temperature FTIR spectra of polymers 1–4 crystallized under two sets of conditions.

was prominent in all of the polymers. The  $\text{tg}^+\text{tg}^-$  conformation of the  $\alpha$  phase has always been a minority, and there was nearly no sign of the  $\text{t}_{m>4}$  conformation of the  $\beta$  phase in polymers 1 and 2 under both crystallization conditions. Polymers 3 and 4 crystallized from solution at 35°C and formed a certain amount of  $\text{t}_{m>4}$  conformation chains, which slightly disappeared after annealing. The FTIR results suggest that the crystalline form of the terpolymers changed from the  $\beta$  phase to the  $\gamma$  phase rather than the  $\alpha$  phase upon introduction of bulky CTFE units. This was consistent with earlier studies.<sup>25</sup> On the other hand, the molecule chains could keep more trans conformation states when the terpolymers were crystallized from the solution at 35°C. This supported the XRD analysis.

### DSC analysis

The DSC curves of the polymers crystallized under two sets of conditions are given in Figure 6. In the high-temperature region, annealed polymers 2 and 3 had two melting peaks in their DSC traces; this indicated the presence of two types of crystals, which was discussed in XRD Analysis section. Morphologically, the shape of the melting peak for polymer 4 crystallized at 35°C was complex (shown as two resolved peaks); this showed that it had complicated crystalline organizations, which may have included a mixture of crystalline structures with different phases and varied size. In fact, the XRD data suggested that all of the polymers crystallized at 35°C should have contained more than one type of crystalline structure; yet, we could only find the single and broad melting peaks in polymers 1–3 crystallized at 35°C, probably because the varied structures in them were at a fully mixed state. In the low-temperature region, there was no obvious phase

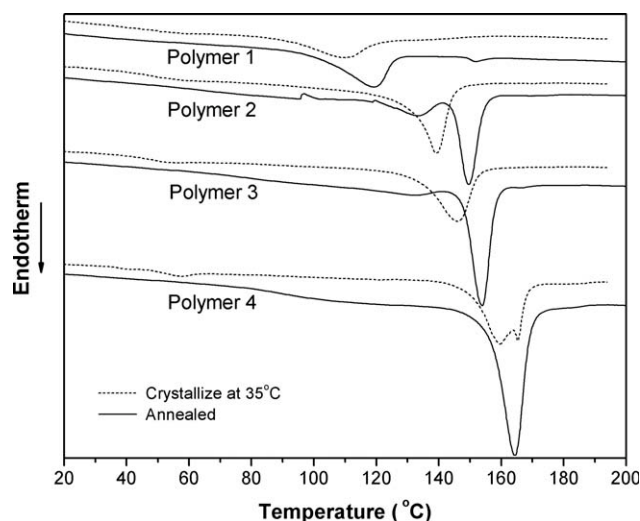


**Figure 6** First-heating DSC traces of polymers 1–4 crystallized under two sets of conditions.

transition in any of the annealed polymers. However, for the samples crystallized from the solutions at 35°C, a weak F–P transition was found in polymers 3 and 4; this confirmed the existence of a small amount of  $\beta$  phase in them. Table IV summarizes the melting transition and phase transition data.

The melting temperature and enthalpy increased with the decrease in the CTFE content of the terpolymer. The polymers crystallized at 35°C showed broad melting peaks with low fusion enthalpies, whereas the annealed polymers exhibited sharp melting peaks with higher fusion enthalpies; this indicated more perfect and larger crystals in the annealed polymers with narrow crystal size distributions. This agreed with the increased crystallite size and enhanced crystallinity calculated based on the XRD patterns. Generally, the annealed polymers had higher melting temperatures, mainly because of their larger crystal size. Nevertheless, other factors affecting the polymer's melting temperature should not be neglected, at the suggestion of the Thompson–Gibbs equation<sup>38</sup>:

$$T_m = T_m^0 \left( 1 - \frac{2\sigma_e}{L\Delta H_f} \right) \quad (6)$$

where  $T_m$  is the melting temperature of the polymer,  $T_m^0$  and  $\Delta H_f$  are the equilibrium melting temperature and enthalpy, respectively, for the same polymer (they can be regarded as constants);  $\sigma_e$  is the surface energy of the folding surface; and  $L$  is the thickness of the polymer lamella. On the basis of the data in Tables III and IV, polymer 1 had the smallest increase in crystal size but a relatively large increase in melting temperature. This suggested that the influence of  $\sigma_e$  should be duly taken into account in this case.

## CONCLUSIONS

In this work, four P(VDF-*ter*-CTFE-*ter*-TrFE) terpolymers containing 68 mol % VDF and different CTFE contents were prepared by partial reduction of chlorine in P(VDF-*co*-CTFE) copolymers. The four P(VDF-*ter*-CTFE-*ter*-TrFE) terpolymers were subsequently allowed to crystallize under two sets of conditions: (1) dissolved in DMF and then crystallized from the solution *in vacuo* at 35°C and (2) annealed at temperatures 5°C below their respective melting temperatures. With XRD, FTIR, and DSC characterizations, we found that the CTFE content and crystallization conditions affected the crystallization behavior of the terpolymers. Because of the large van der Waals radius of chlorine in the CTFE units and their random distribution along the polymer chains, the increased CTFE content made the terpolymers contain less  $\beta$  phase (it even disappeared), which had closely packed  $t_{m>4}$  conformation chains. More  $\gamma$  phase with loosely packed  $tttg^+tttg^-$  conformation chains was found in them, and it became prominent. The CTFE unit, acting as the defect, destroyed the crystalline structure, reduced the crystal size, and lowered the crystallinity, fusion enthalpy, and melting temperatures of the terpolymers. On the other hand, probably because in the

**TABLE IV**  
Summary of the DSC Data for the Polymers Crystallized Under Two Sets of Conditions

Polymer $j$	Crystallized at 35°C				Annealed			
	$T_m$ (°C)	$\Delta H_m$ (J/g)	$T_c$ (°C)	$\Delta H_c$ (J/g)	$T_{m1}$ (°C)	$\Delta H_{m1}$ (J/g)	$T_{m2}$ (°C)	$\Delta H_{m2}$ (J/g)
1	110.2	−5.28	NA	NA	119.2	−9.27	NA	NA
2	139.2	−11.32	NA	NA	133.1	−2.51	149.7	−8.77
3	145.8	−11.80	53.9	−0.52	136.2	−0.95	154.0	−13.05
4	162.9 <sup>a</sup>	−13.61	57.5	−0.86	164.3	−22.8	NA	NA

$\Delta H_c$ , enthalpy corresponding to the F–P transition;  $\Delta H_m$ , enthalpy associated with the melting behavior; NA, not available;  $T_c$ , peak temperature corresponding to the F–P transition;  $T_m$ , peak temperature associated with the melting behavior.

<sup>a</sup> The average temperature of the two resolved melting peaks in the DSC trace of polymer 4 crystallized at 35°C.



solution the polymer chains were more expanded with a less helical structure, which resulted in closer packing of the molecular chains containing more trans conformation in the crystals, the terpolymers crystallized from the solution at 35°C included more polar components compared with the corresponding annealed ones. However, the annealed polymers had higher crystallinities, melting temperatures, and fusion enthalpies and larger crystal sizes, mainly because of better molecular mobility at the higher crystallization temperature; this made the crystal structure easier to perfect.

## References

1. Lovinger, A. J. *Science* 1983, 220, 1115.
2. Wang, T. T.; Herbert, J. M.; Glass, A. M. *The Application of Ferroelectric Polymers*; Blackie/Chapman & Hall: New York, 1988.
3. Naber, R.; Tanase, C.; Blom, P.; Gelinck, G. H.; Marsman, A. W.; Touwslager, F. J.; Setayesh, S.; de Leeuw, D. M. *Nat Mater* 2005, 4, 243.
4. Stadlober, B.; Zirkl, M.; Beutl, M.; Leising, G. *Appl Phys Lett* 2005, 86, 242902.
5. Chu, B.; Zhou, X.; Ren, K.; Neese, B.; Lin, M.; Wang, Q.; Bauer, F.; Zhang, Q. M. *Science* 2006, 313, 334.
6. *Electroactive Polymer (EAP) Actuators as Artificial Muscles*; Bar-Cohen, Y., Ed.; SPIE: Bellingham, WA, 2004.
7. Ameduri, B. *Chem Rev* 2009, 109, 6632.
8. Ameduri, B.; Boutevin, B. *Well-Architected Fluoropolymers: Synthesis, Properties and Applications*; Elsevier: Amsterdam, 2004.
9. Scheirs, J. *Modern Fluoropolymers*; Wiley: New York, 1997.
10. Hasegawa, R.; Takahashi, Y.; Chatani, Y.; Tadokoro, H. *Polym J* 1972, 3, 600.
11. Lovinger, A. J.; Furukawa, T.; Davis, G. T.; Broadhurst, M. G. *Polymer* 1983, 24, 1225.
12. Yagi, T.; Tatemoto, M.; Sako, J. *Polym J* 1980, 12, 209.
13. Davis, G. T.; Furukawa, T.; Lovinger, A. J.; Broadhurst, M. G. *Macromolecules* 1982, 15, 329.
14. Higashihata, Y.; Sako, J.; Yagi, T. *Ferroelectrics* 1981, 32, 85.
15. Tajitsu, Y.; Chiba, A.; Furukawa, T.; Date, M.; Fukada, E. *Appl Phys Lett* 1980, 36, 286.
16. Yamada, T.; Ueda, T.; Kitayama, T. *J Appl Phys* 1981, 52, 948.
17. Chung, T. C.; Petchsuk, A. *Proc SPIE* 2001, 4329, 117.
18. Xu, H.; Cheng, Z.; Olson, D.; Mai, T.; Zhang, Q. M.; Kavarnos, G. *Appl Phys Lett* 2001, 78, 2360.
19. Chung, T. C.; Petchsuk, A. *Macromolecules* 2002, 35, 7678.
20. Xia, F.; Cheng, Z. Y.; Xu, H.; Li, H.; Zhang, Q. M.; Kavarnos, G. J.; Ting, R. Y.; Abdel-Sadek, G.; Belfield, K. D. *Adv Mater* 2002, 14, 1574.
21. Xu, H.; Shen, D.; Zhang, Q. M. *Polymer* 2007, 48, 2124.
22. Feiring, A. E.; Hulburt, J. D. *Chem Eng News* 1997, 75, 6.
23. Lu, Y. Y.; Claude, J.; Neese, B.; Zhang, Q. M.; Wang, Q. *J Am Chem Soc* 2006, 128, 8120.
24. Wang, Z. M.; Zhang, Z. C.; Chung, T. C. *Macromolecules* 2006, 39, 4268.
25. Lu, Y. Y.; Claude, J.; Zhang, Q. M.; Wang, Q. *Macromolecules* 2006, 39, 6962.
26. Zhang, Z. C.; Chung, T. C. *Macromolecules* 2007, 40, 783.
27. Claude, J.; Lu, Y. Y.; Li, K.; Wang, Q. *Chem Mater* 2008, 20, 2078.
28. Zhang, Z. C.; Meng, Q. J.; Chung, T. C. *Polymer* 2009, 50, 707.
29. Lu, Y. Y.; Claude, J.; Norena-Franco, L. E.; Wang, Q. *J Phys Chem B* 2008, 112, 10411.
30. Zhao, C.; Guo, M.; Lu, Y. Y.; Wang, Q. *Macromol Symp* 2009, 279, 52.
31. Harrowven, D. C.; Guy, I. L. *Chem Commun* 2004, 1968.
32. Yagi, T.; Tatemoto, M. *Polym J* 1979, 11, 429.
33. Zhang, Q. M.; Xu, H. S.; Fang, F.; Cheng, Z.; Xia, F.; Hou, Y. *J Appl Phys* 2001, 89, 2613.
34. Fang, F.; Zhang, M. Z.; Huang, J. F. *J Polym Sci Part B: Polym Phys* 2005, 43, 3255.
35. Salimi, A.; Yousefi, A. A. *J Polym Sci Part B: Polym Phys* 2004, 42, 3487.
36. Reynolds, N. M.; Kim, K. J.; Chang, C.; Hsu, S. L. *Macromolecules* 1989, 22, 1092.
37. Kim, K. J.; Kim, G. B.; Valencia, C. L.; Rabolt, J. F. *J Polym Sci Part B: Polym Phys* 1994, 32, 2435.
38. Marand, H.; Hoffman, J. D. *Macromolecules* 1990, 23, 3682.